For submission to the Bulletin of the Seismological Society of America

Seismic input motion determined from a surface-downhole pair of sensors: a constrained deconvolution approach.

Bindi[1], D., Parolai, S.[2], Picozzi, M.[2], Ansal, A.[3]

[1]Istituto Nazionale di Geofisica e Vulcanologia, Via Bassini 15, 20133 Milano Italy
[2]Deutsches GeoForschungsZentrum GFZ, Section 2.1, Telegrafenberg, 14473 Potsdam, Germany
[3]Boğaziçi Üniversitesi, Kandilli Rasathanesi ve Deprem Araştırma Enstitüsü, Department of Earthquake Engineering, 34684, Çengelköy, Istanbul, Turkey

Abstract

We apply a deconvolution approach to the problem of determining the input motion at the base of an instrumented borehole using only a pair of recordings, one at the borehole surface and the other at its bottom. To stabilize the bottom-to-surface spectral ratio, we apply an iterative regularization algorithm that allows us to constrain the solution to be positively defined and to have a finite time duration. Through the analysis of synthetic data, we show that the method is capable of retrieving reliable input motion, suppressing the effect of the negative interference generated by the down-going waves. Results obtained by applying the methodology to weak earthquakes recorded at the Ataköy (Istanbul) vertical array are also presented and show that removing the effect of the down-going waves is remarkable, even considering the recording at a depth of 140 m.

Introduction

We address the problem of determining the input motion at the bottom of a borehole when both the surface and down-hole recordings of an earthquake are available. We consider the case of a layered medium with small impedance contrasts and we limit our attention to small deformation that would lead to a linear relationship between

stress and strain. Indeed, the considered approach is valid under the same conditions required for describing soil non-linearity in terms of a linear equivalent model that is for the case of time independent stress-strain relationships. The determination of the site transfer function of homogenous or stratified one-dimensional (1D) model using a pair of records has been extensively discussed in several previous works (e.g. Safak, 1997). In this work, except for the assumption of an absence of any strong impedance contrasts capable of generating significant reflections and refractions in the wave field, knowledge of vertical profiles of typical geophysical/geotechnical parameters is not required. The problem of determining the input motion is not trivial since both the surface and the down-hole recordings cannot be directly used, since the former are affected by site effects related to the propagation from the bottom to the top of the borehole, and the latter are contaminated by waves reflected by the free surface. The approach we follow belongs to the so-called down-hole array seismogram inversion (e.g., Metha et al., 2007; Assimaki et al., 2008; Parolai et al., 2009a), in which the Green's function between the bottom of the borehole and the free surface is empirically determined by deconvolving the surface recording with the down-hole one.

We first describe the regularization scheme used to perform the deconvolution, based on the Landweber method (e.g Bertero and Boccacci, 1998). The proposed iterative scheme is validated through the analysis of synthetic data generated using the velocity profile previously determined for the Ataköy vertical array (Parolai et al., 2009a). The role played by the a-priori constraints introduced in the regularization scheme is discussed as well. Finally, some earthquakes recorded by sensors located at different depths of the Ataköy vertical array are used as examples to perform the constrained deconvolution.

Method

The problem discussed in this work is sketched out in Figure 1, where S(t) and B(t) represent the ground motion recorded at the surface and at the base of the borehole, respectively, while I(t) is the input seismic waveform. The problem is therefore how to determine I(t) given S(t) and B(t), without requiring any knowledge of the soil profile. Considering the symbol * to indicate the usual convolution product between two functions (i.e. $(f * g)(\tau) = \int_{-\infty}^{+\infty} f(t)g(\tau - t)dt$), the relation between these signals can be written in symbolic notation as

$$S = 2I * P_U \qquad (1)$$

and

$$B = I + 0.5S * P_D = I + (I * P_U) * P_D = I + I * (P_U * P_D) = I + I * P_T \qquad (2)$$

where P_U and P_D represents the propagator for waves traveling from the base to the surface and vice versa, respectively, (right panel in Figure 1). In equation 1 the factor 2 accounts for the free-surface effects (assuming vertical incidence). In equation (2), the associative properties of the convolution product have been used to define the total propagator P_T. The dependence on time has been omitted for the sake of simplicity.

Following the downhole seismogram inversion approach, the signal *S(t)* recorded at the surface is deconvolved from the downhole recording *B(t)* to determine the propagator from the surface to the base of the borehole. Considering that in the Fourier domain $\hat{F}(\omega) = \int_{-\infty}^{+\infty} f(t)e^{-i\omega t}dt$ represents the Fourier transform of *f(t)*, the above described operation corresponds to computing the following ratio

$$\frac{\hat{B}}{\hat{S}} = \frac{\hat{I} + \hat{I}\hat{P}_T}{2\hat{I}\hat{P}_U} = \frac{1 + \hat{P}_T}{2\hat{P}_U} = \frac{1}{2\hat{P}_U} + \frac{\hat{P}_D}{2} \tag{3}$$

Note that in equation (3), we have omitted the dependence on the angular frequency ω for the sake of simplicity. Equation (3), which represents the transfer function of a linear system with feed-back, stresses the contamination of $\hat{B}$ with signals reflected from the free surface and that are propagated down by $\hat{P}_D$. Hereinafter, we will refer to propagation from the bottom to the surface as up-going propagation, and from the surface towards the base as down-going. Hence, the aim of this work is to estimate *I(t)* starting from the ratio shown in equation (3) and mitigating the effect of down-going propagation. In fact, in the case that the term related to $\hat{P}_D$ is negligible, the ratio $\hat{B}/\hat{S}$ provides an estimate of $\hat{P}_U$ that, in turn, can be removed from $\hat{S}$ to estimate $\hat{I}$.

Two problems, however, arise: first, the ill-posed nature of the deconvolution considered as an inverse problem, and second, the effect of down-going waves. To mitigate the effects of the numerical instabilities amplified by the spectral ratio, we apply a regularization method whereas the effect of down-going waves is filtered out by introducing some constraints to the solution. We consider an iterative method, known as the Landweber method (e.g. Bertero and Boccacci, 1998), based on a successive approximation scheme. This method has been modified by Bertero et al. (1997) to include a-priori constraints on the solutions, leading to the following iterative scheme

$$f_{n+1} = P_C\left[f_n + \alpha S^T * (B - S * f_n)\right] \tag{4}$$

where *Pc* denotes the convex projection onto the closed and convex set C, *n* is the number of the completed iterations, f_n is the regularized solution at iteration *n*, $S^T(t)=S(-t)$, and α is a relaxation parameter that must satisfy the following condition

$$0 < \alpha < \frac{2}{\hat{S}_{\max}^2} \qquad \hat{S}_{\max} = \max_{\omega} \left| \hat{S} \right| \tag{5}$$

A suitable choice of α can be $\alpha=1/\hat{S}_{\max}^2$. The iteration scheme (4) is generally initialized by taking $f_0=0$ (e.g. Lanza et al., 1999; McGuire, 2004; Liao and Huang, 2008) and the relevant convergence results are described in Eicke (1992). The projection *Pc* in equation (4) is used to introduce some a-priori constraint on the solution. Since we aim to suppress the effect of the down-going waves whose propagator is defined by a causal signal, we consider as C the set of a-causal and positive functions. Furthermore, to avoid artifacts in the deconvolution, we select a time frame outside of which the propagator is set to zero. This time frame, hereinafter referred to as propagator domain or support, is visually selected by performing the inversion twice, first without applying the constraints to visually evaluate the propagator domain, and then by applying the full set of constraints.

The number of iteration *n* acts as regularization parameter. In particular, solutions corresponding to low values of *n* are strongly filtered, while the instabilities affecting the solution increase with increasing *n*. In the case of the synthetic test, the optimal value of *n* can be determined by comparing the true solution with the regularized ones. In the case of real data, several strategies can be applied to estimate this optimal value, considering that the projected Landweber method shows the usual semi-convergence property of the regularizing iterative methods: the restoration error decreases first and increases afterwards, i.e. the restoration error has a minimum corresponding to a certain number of iterations (Eicke, 1992; Bertero and Boccacci,

1998). We therefore estimate the optimal number of iterations by analyzing the so called L-curve, constructed by evaluating, for each *n,* the residual between the observations and the reconstructions, and the size of the regularized solution.

Application to synthetic data

The performance of the projected Landweber is evaluated through the analysis of synthetic data. Synthetic seismograms are calculated using a layered subsoil velocity model derived for the vertical array in Ataköy (Istanbul) (Parolai et al., 2009a). This model was shown to provide deconvolved wavefield pulse arrivals consistent with those observed with real data. The average apparent quality factors for S-waves have been recently estimated by a spectral fitting procedure coupled with a down-hole array inversion (Parolai et al., 2009b). However, since their values do not affect the validity of the tests, the quality factors for both P and S-waves, as well as the soil-structure densities, were assigned standard values found in the literature that are suitable for near-surface soft geological material. The synthetic seismogram calculation is carried out using a matrix propagator method (Wang, 1999), with the source located at a depth of 10 km and at an epicentral distance of 10 km from the borehole. The model is described in detail in Parolai et al., (2009b, their Table 1). The synthetic recordings are computed at both 50m depth and surface and then corrupted with seismic noise recorded in Ataköy at the same depths (50m and 0m depth, respectively).

The synthetic seismograms are shown in Figure 2. The full surface to down-hole propagator, describing both the effects of up-going (a-causal) and down-going (causal) waves, is shown in the bottom-left panel. This propagator has been obtained by applying the Landweber method without constraining the down-hole to surface

ratio. It has been previously shown that the application of the Landweber without constraints provides results very similar to those achieved by applying crude regularization techniques based on water-level criteria (e.g. Bertero et al., 1997; Parolai et al., 2009a). The results obtained by constraining the solution are shown in the right frames of Figure 2. The time domain of the solution is selected by visual inspection of the unconstrained solution. We constrain the support to start at -0.22 s and, since we wish to suppress the effect of the down-going waves, to end at -0.05 s. Then, the deconvolution is performed by looking for solutions which are positive within the support (gray area in bottom-right panel of Figure 2) and zero outside. In the top-right frame of Figure 2, the seismogram reconstructed at 50 m by convolving the constrained solution with the surface recording is compared to the synthetic seismogram computed avoiding the generation of down-going waves, with very good agreement being observed. The solution shown in Figure 2 has been obtained setting the number of iterations to 50. This value has been chosen by computing the L-curve (left panel in Figure 3) and selecting the number of iterations corresponding to the point of maximum curvature (Hansen et al., 2007).

Figure 3 (right panel) compares the Fourier spectra of the recordings at the bottom and surface of the borehole with the spectra of both the unconstrained and constrained solution. The Landweber filter in the spectral domain is also shown. The down-hole spectrum (bottom) shows the typical troughs of the down-hole recording caused by negative interference generated by the down-going waves, which are absent in the surface spectrum. Since the Landweber filter is tied to the denominator of the spectral ratio, i.e. the surface spectrum, it shows a pass-band shape, regularizing low and high frequencies, because they have small values in the surface recording spectrum. The frequencies corresponding to the troughs are not regularized since this feature is

related to the numerator of the spectral ratio. In the absence of any constraints, the regularization method is linear and then the spectrum of the unconstrained solution shows the typical troughs affecting the down-hole spectrum. Moreover, the band width of the solution is determined by the Landweber filter and, hence, it is controlled by the bandwidth of the surface spectrum. Since at both low and high frequencies this spectrum vanishes, the spectrum of the propagator will also vanish. This means, for example, that the area under the up-going pulse cannot be restored. On the other hand, since the positivity constraint makes the scheme non-linear, the band-width of the deconvolution can be extrapolated outside the band-width of the Landweber filter. In the case of image restoration, this effect is known as super resolution and is due to the possibility of extrapolating the Fourier transform of a band-limited image when the support of the image is known (Bertero and De Mol, 1996). Then, a priory information (i.e. a positive solution with finite duration) applied as constraints to the regularized solution allows us to partially retrieve information about propagation both at low and high frequencies.

Finally, in order to evaluate the reliability of the proposed approach, the input ground motion is estimated by following the standard engineering practice (e.g. Figini and Paolucci, 2009), where the effect of up-going propagation is removed from the ground motion observed at the surface by considering the theoretical Green's function computed for the analyzed model. To accomplish this task, we used the EERA software (Bardet et al., 2000), by setting to one the number of iterations relevant to the linear-equivalent scheme. The results obtained with EERA and by applying the projected Landweber method are compared to the synthetic seismogram in Figure 4. A generally good agreement is observed between the solutions provided by EERA

and projected Landweber methods, both being able to suppress the effect of down-going waves.

However, the amplitude of the Landweber solution is closer to the target input. The EERA deconvolution was carried out by limiting the number of iterations to 1, that is, in agreement with the linear forward calculation of the seismograms and, not allowing the modification of the starting velocities and damping values. Nonetheless, a lower degree of reconstruction of the target input was obtained. This might indicate that the choice of the starting parameters, even if chosen considering the most suitable ones available in literature, might significantly affect the results.

Note, that this is a quite common situation when dealing with real data either because measured damping values are often not available or because they are affected by larger uncertainties than the velocity values. The observed closeness of the Landweber solution to the target input might also suggest a better regularization behavior of this method with respect the one implemented in EERA. In both cases, a clear advantage of the proposed method with respect to the standard one should be apparent since it allows us both to consider the right amount of damping and to optimize the regularization in the deconvolution operation.

Application to observed data

The projected Landweber method is applied to the surface-downhole pair of recordings of two small earthquakes recorded by the Ataköy vertical array (Parolai et al., 2009a). Figure 5 shows the deconvolutions obtained considering two earthquakes of magnitude 4.6 and 4.4 that occurred in the Marmara Sea. The constrained deconvolution is applied considering the surface recording and down-hole recordings at two different depths, 50 m and 140 m, respectively. The obtained propagator is

used to compute the input motion at the bottom of the borehole, avoiding the effect of the down-going waves. The results for one of the two earthquakes are shown in Figure 6, in both the time and frequency domains. The ratio between the down-hole and surface Fourier amplitude spectra, which are shown in the top-left panel, is characterized by the presence of spectral troughs related to the negative interference generated by the down-going wave (top-right frame). The spectrum of the constrained propagator (black line in the top-right frame) is smoother, but in the high-frequency range its band-width is limited by the information contained in the surface spectrum. Hence, spectral information at high frequencies lost during the up-going propagation due anelastic attenuation cannot be restored. The comparison between the down-hole recording and the input motion estimated through the deconvolution is shown in the bottom frames of Figure 6, in the frequency (left) and time (right) domains. We note, when comparing the differences between the estimated input and down-hole recorded ground motion, in both the time and frequency domains, that removing the effect of the down-going waves is remarkable, even considering the recording at a depth of 140 m.

Conclusions

We proposed a constrained regularization scheme for performing a deconvolution within the framework of down-hole array inversion. This scheme, when applied to a surface and down-hole pair of recordings, is effective in restoring the input motion at the bottom, while mitigating the effect of down-going waves. In comparison to the standard approach of determining the input motion by computing numerically the transfer function for the considered model, this approach has the advantage of not requiring any knowledge of the soil structure. Therefore, it can be applied to any

borehole array where the soil structure is not known. Moreover, it can be used to verify the reliability of any simplification carried out when averaging the borehole profiles derived by downhole or PS-logging measurements. In this work, we evaluated the effectiveness of the constrained deconvolution by considering an almost homogeneous medium and a linear model. The case of either non-linear soil behavior or propagation within a medium characterized by sharp changes of velocity will be the subject of future work, either exploiting the database of earthquakes that have been/will be recorded by the Ataköy vertical array (western Istanbul) or developing ad-hoc simulations. However, we remark that the proposed method is equivalent to an equivalent-linear approach, that is to an approach in which the stress-strain relationship is not time-dependent and the velocities and damping values in each layer are adjusted depending only on the magnitude of the input ground motion or, in the case of downhole array seismogram inversion (Assimaki et al., 2008), adjusted with respect to a starting value to fit the observed data. Under these conditions, the empirical Green's function can approximate soil non-linearity.

Finally, since the positive constraint applied to the solution could allow us to better restore the area and the width of the propagation pulse, future efforts will be devoted to investigating how to exploit these improvements on the restored pulse to study attenuation properties.

Data and Resources

EERA Software is available on internet site:

http://gees.usc.edu/GEES/Software/EERA2000/ (last access on September 2009)

The figures in this work have been drawn with the GMT software (Wessel and Smith, 1991)

Acknowledgments

We would like to thank the Associate Editor Diane I. Doser for her comments and suggestions that allowed us to significantly improve the manuscript. We also thank an anonymous reviewer for having pointed out one error in a previous version of Figure 6. K. Fleming kindly improved our English. One of the authors (D.B.) did this work during a 1 yr stay at the GFZ, Potsdam.

References

Assimaki, D., W. Li, J. H. Steidl, and K. Tsuda (2008), Site amplification and attenuation via downhole array seismogram inversion: a comparative study of the 2003 Miyagi-Oki aftershock sequence. Bull. Seism. Soc. Am. 98, 301-330.

Bardet, J. P., Ichii, K., and Lin, C. H. (2000). EERA, A computer program for equivalent-linear earthquake site response analyses of layered soil deposits, University of Southern California, August 2000.

Bertero M., and C. De Mol (1996). Super-resolution by data inversion, Progress in Optics, vol XXXVI, edit by E Wolf (Amsterdam: Elsevier), 129–178

Bertero,M., D. Bindi, P. Boccacci, M. Cattaneo, C. Eva and V. Lanza (1997). Application of the projected Landweber method to the estimation of the source time function in seismology, Inverse Problems, 13, 465-486.

Bertero, M. and P. Boccacci (1998). Introduction to inverse problems in imaging. Bristol:IOP Publishing.

Eicke, B., (1992). Iteration methods for convexly constrained ill-posed problems in Hilbert space, Funct. Anal. Optimiz., 13, 413-429.

Figini, R. and R. Paolucci (2009). Site Effects at Long Periods from Digital Strong Motion Records of the KiK-net, Japan, Journal of Earthquake Engineering, 13, 567-584

Hansen, C., T. K. Jensen, and G. Rodriguez (2007) An adaptive pruning algorithm for the discrete L-curve criterion. Journal of Computational and Applied Mathematics 198 , 2, 483 - 492 ISSN:0377-0427

Lanza,V., D. Spallarossa, M. Cattaneo, D. Bindi and P. Augliera (1999). Source parameters of small events using constrained deconvolution with empirical Green's functions, Geophys. J. Int., 137, 651-662

Liao, B-Y., and H-C Huang (2008). Rupture Process of the 2002 Mw 7.9 Denali Earthquake, Alaska, Using a Newly Devised Hybrid Blind Deconvolution Method, Bull. Seism. Soc. Am. 98, 162-179 DOI: 10.1785/0120050065

McGuire, J.J. (2004) Estimating Finite Source Properties of Small Earthquake Ruptures, Bull. Seism. Soc. Am. 94. 377-393; DOI: 10.1785/0120030091

Mehta, K., R. Snieder, and V. Grazier (2007). Downhole receiver function: a case study. Bull. Seism. Soc. Am. 97, 1396-1403

Parolai, S., A. Ansal, A. Kurtulus, A. Strollo, R. Wang and J. Zschau (2009a). The Ataköy vertical array (Turkey): insights into seismic wave propagation in the shallow-most crustal layers by waveform deconvolution, Geophys. J. Int. doi:10.1111/j.1365-246X.2009.04257.x

Parolai, S., D. Bindi, A. Ansal, A. Kurtulus , A. Strollo, and J. Zschau (2009b) Determination of shallow S-wave attenuation by down-hole waveform deconvolution: a case study in Istanbul (Turkey), submitted to Geophys. J. Int.

Safak, E. (1997). Models and methods to characterize site amplification from a pair of records. Earthquake Spectra, 13, 97-129

Wang, R., (1999). A simple orthonormalization method for stable and efficient computation of Green's functions. Bull. Seism. Soc. Am. 89, 733-741.

Wessel, P., and W. H. F. Smith (1991). Free software helps map and display data, EOS 72, no. 41, 441, 445–446.

Figure captions

Figure 1. Sketch of the considered problem. Left: the surface recording S(t) and the down-hole recording B(t) are used to determine the input recording I(t). Right: the up-going and down-going wave propagation is described using a linear system having transfer functions equal to P_U and P_D, respectively.

Figure 2 Results for synthetic tests. Left: unconstrained deconvolution. Right: deconvolution with positivity and domain constraints. Top: down-hole recording (50 m depth); middle: surface recording; bottom: results of the down-hole to surface deconvolution, with amplitudes scaled to the sampling rate value (i.e., 200). In the top right panel, the comparison between the estimated input recording (black) and the target one (gray) is also shown.

Figure 3 Left: Example of a L-curve estimated for the synthetic test shown in Figure 2. The l-2 norm of the solution is shown against the norm of residuals for different number of iterations (circle). Right: Fourier amplitude spectra of the surface (black) and down-hole (gray) recordings. The spectra of the bottom-to-surface deconvolution is also shown, with (dashed black) and without (dashed gray) considering the constraints. The Landweber filter is also shown (dotted). Note that the numerical scale on the y-axis is the same for the spectra of the recordings and the deconvolutions, but the units are relevant only to the recordings.

Figure 4 Comparison between the synthetic input motion (gray) and the reconstructions obtained by applying the constrained deconvolution approach (black)

and the EERA software (dotted). The simulated down-hole recording (dashed) is also shown for comparison

Figure 5. Results of the down-hole to surface deconvolution performed when considering the recordings of two earthquakes at the Ataköy vertical array (see Parolai et al. 2009 a for details about the event). Two different sensor depths are considered (140m on the left and 50 m on the right). The solutions obtained without applying any constraints (gray) are compared to the constrained ones (black). The amplitudes of the deconvolutions are scaled to the sampling rate value (i.e., 200).

Figure 6 Constrained deconvolution analyses for one of the two earthquakes shown in Figure 5 (eq080312, bottom panels). The considered borehole depth is 140 m. Top left: Fourier amplitude spectra of the surface (black) and down-hole (gray) recordings. Top right: Spectral ratio between the bottom and surface recordings (gray) and spectrum of the constrained Landweber solution (black). Bottom left: comparison between the spectrum of the down-hole recording (gray) and the restored one by deconvolution (black). Bottom right: comparison between the time series, extracted around the S-wave arrivals, of the down-hole (gray) and that computed by deconvolution (black) recordings.

Figures

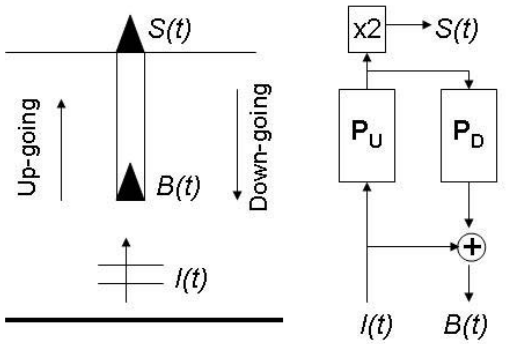

Figure 1. Sketch of the considered problem. Left: the surface recording S(t) and the down-hole recording B(t) are used to determine the input recording I(t). Right: the up-going and down-going wave propagation is described using a linear system having transfer functions equal to P_U and P_D, respectively.

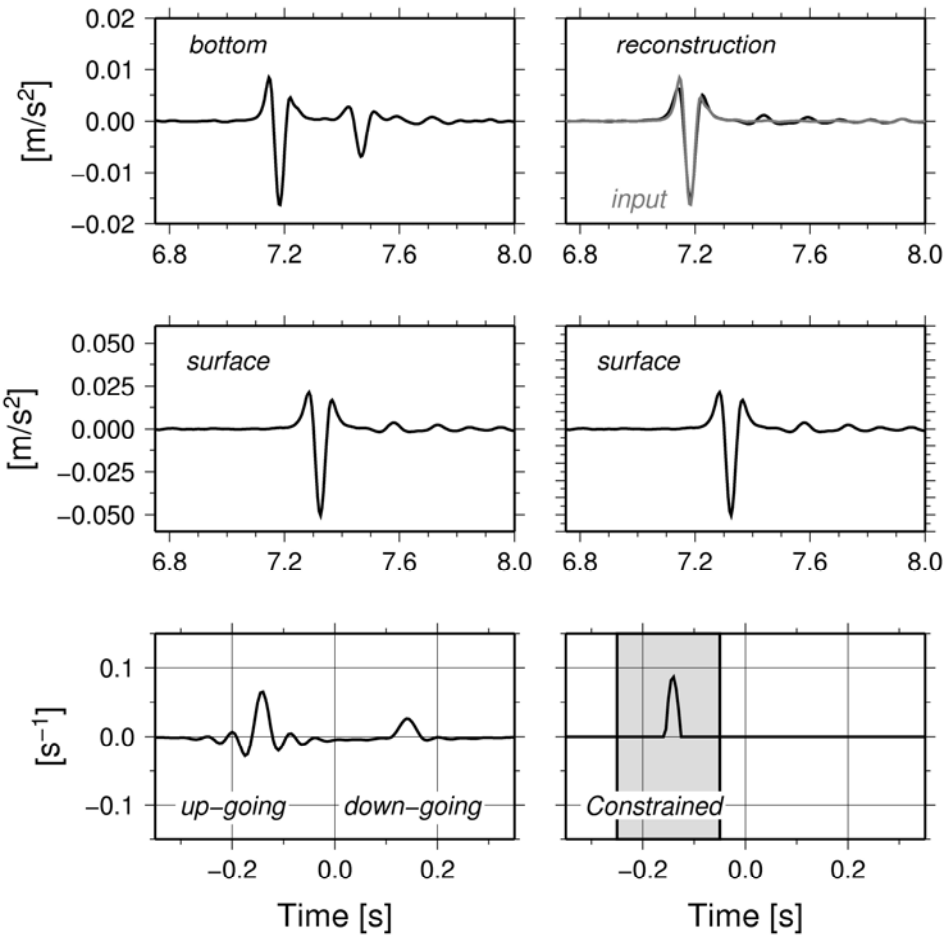

Figure 2 Results for synthetic tests. Left: unconstrained deconvolution. Right: deconvolution with positivity and domain constraints. Top: down-hole recording (50 m depth); middle: surface recording; bottom: results of the down-hole to surface deconvolution, with amplitudes scaled to the sampling rate value (i.e., 200). In the top right panel, the comparison between the estimated input recording (black) and the target one (gray) is also shown..

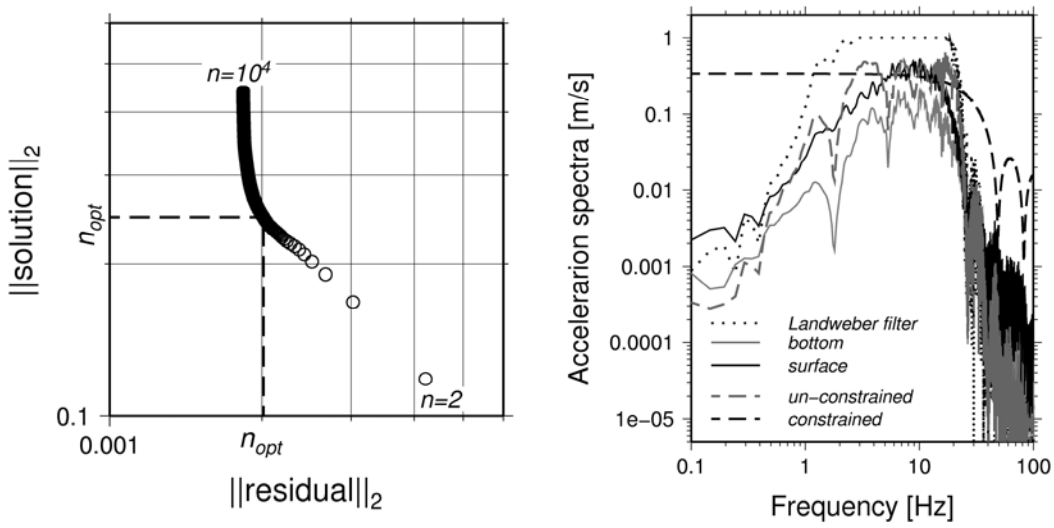

Figure 3 Left: Example of a L-curve estimated for the synthetic test shown in Figure 2. The l-2 norm of the solution is shown against the norm of residuals for different number of iterations (circle). Right: Fourier amplitude spectra of the surface (black) and down-hole (gray) recordings. The spectra of the bottom-to-surface deconvolution is also shown, with (dashed black) and without (dashed gray) considering the constraints. The Landweber filter is also shown (dotted). Note that the numerical scale on the y-axis is the same for the spectra of the recordings and the deconvolutions, but the units are relevant only to the recordings.

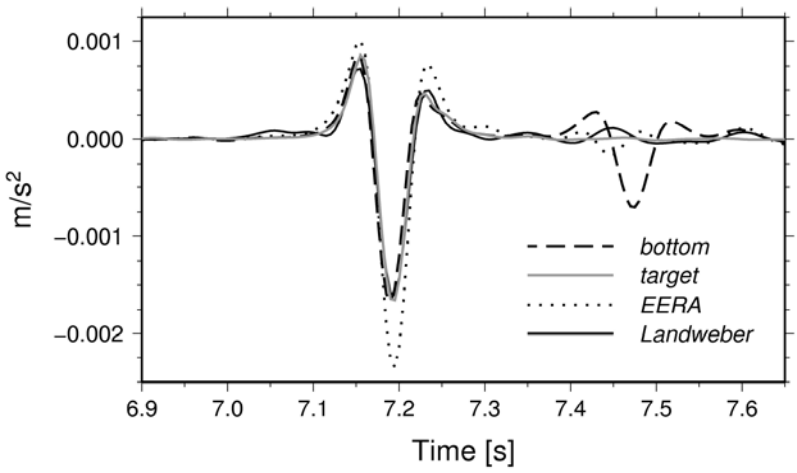

Figure 4 Comparison between the synthetic input motion (gray) and the reconstructions obtained by applying the constrained deconvolution approach (black) and the EERA software (dotted). The simulated down-hole recording (dashed) is also shown for comparison

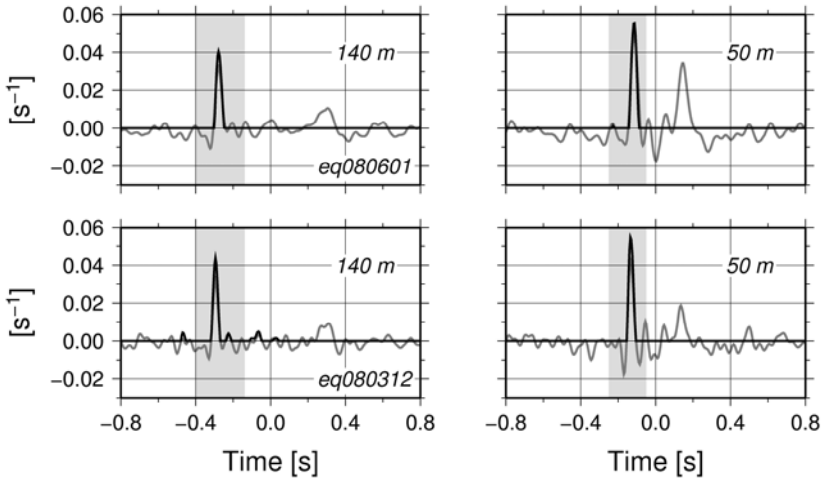

Figure 5. Results of the down-hole to surface deconvolution performed when considering the recordings of two earthquakes at the Ataköy vertical array (see Parolai et al. 2009 a for details about the event). Two different sensor depths are considered (140m on the left and 50 m on the right). The solutions obtained without applying any constraints (gray) are compared to the constrained ones (black). The amplitudes of the deconvolutions are scaled to the sampling rate value (i.e., 200).

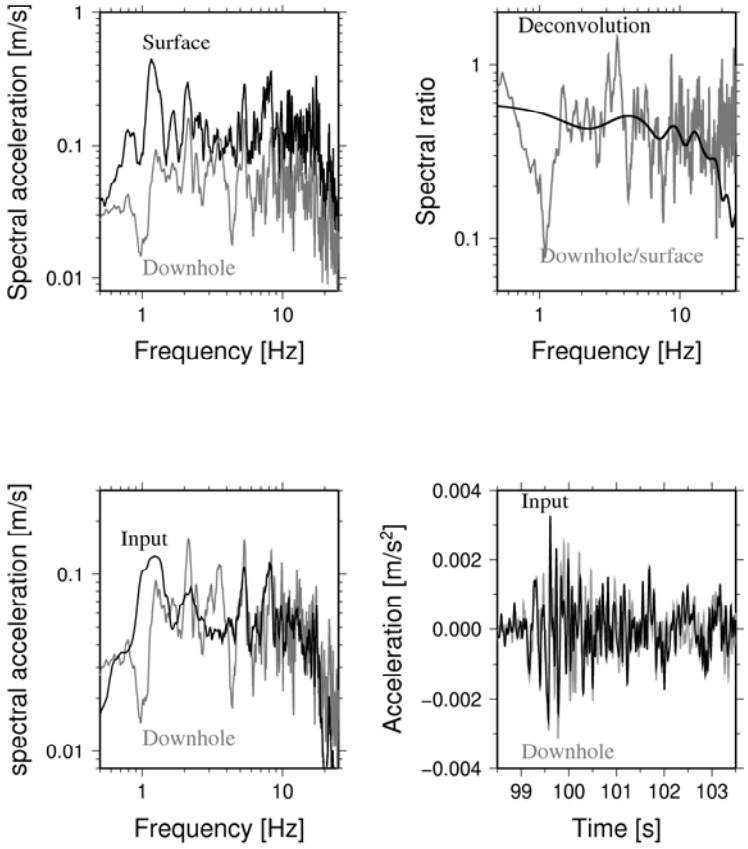

Figure 6 Constrained deconvolution analyses for one of the two earthquakes shown in Figure 5 (eq080312, bottom panels). The considered borehole depth is 140 m. Top left: Fourier amplitude spectra of the surface (black) and down-hole (gray) recordings. Top right: Spectral ratio between the bottom and surface recordings (gray) and spectrum of the constrained Landweber solution (black). Bottom left: comparison between the spectrum of the down-hole recording (gray) and the restored one by deconvolution (black). Bottom right: comparison between the time series, extracted around the S-wave arrivals, of the down-hole (gray) and that computed by deconvolution (black) recordings.